Published in final edited form as:
Science. 2012 November 9; 338(6108): 818–822. doi:10.1126/science.1226191.

IRE1α Cleaves Select microRNAs During ER Stress to Derepress Translation of Proapoptotic Caspase-2

John-Paul Upton[1,7,*], **Likun Wang**[2,6,8,*], **Dan Han**[2,6,8], **Eric S. Wang**[1], **Noelle E. Huskey**[2,7], **Lionel Lim**[2,7], **Morgan Truitt**[3,7], **Michael T. McManus**[4,5], **Davide Ruggero**[3,7], **Andrei Goga**[2,7], **Feroz R. Papa**[2,5,6,8,¶], and **Scott A. Oakes**[1,7,¶]

[1]Department of Pathology, University of California-San Francisco, San Francisco, CA 94143, USA

[2]Department of Medicine, University of California-San Francisco, San Francisco, CA 94143, USA

[3]Department of Urology, University of California-San Francisco, San Francisco, CA 94143, USA

[4]Department of Microbiology and Immunology, University of California-San Francisco, San Francisco, CA 94143, USA

[5]Diabetes Center, University of California-San Francisco, San Francisco, CA 94143, USA

[6]Lung Biology Center, University of California-San Francisco, San Francisco, CA 94143, USA

[7]Helen Diller Comprehensive Cancer Center, University of California-San Francisco, San Francisco, CA 94143, USA

[8]California Institute for Quantitative Biosciences, University of California-San Francisco, San Francisco, CA 94143, USA

Summary

Protein misfolding stimulates a signaling pathway involving noncoding RNAs to promote cell death.

The endoplasmic reticulum (ER) is the primary organelle for folding and maturation of secretory and transmembrane proteins. Inability to meet protein-folding demand leads to “ER stress,” and activates IRE1α, an ER transmembrane kinase-endoribonuclease (RNase). IRE1α promotes adaptation through splicing *Xbp1* mRNA or apoptosis through incompletely understood mechanisms. Here we found that sustained IRE1α RNase activation caused rapid decay of select microRNAs (miRs -17, -34a, -96, -125b) that normally repress translation of *Caspase-2* mRNA, and thus sharply elevates protein levels of this initiator protease of the mitochondrial apoptotic pathway. In cell-free systems, recombinant IRE1α endonucleolytically cleaved microRNA precursors at sites distinct from DICER. Thus, IRE1α regulates translation of a proapoptotic protein through terminating microRNA biogenesis, and noncoding RNAs are part of the ER stress response.

Various physiological events (e.g., secretory cell differentiation, polypeptide hormone production) and pathological insults (e.g., hypoxia, ischemia, changes in intracellular pH) increase protein-folding demand on the secretory pathway to trigger ER stress (1). The tripartite unfolded protein response (UPR) signaling arms of IRE1α, PERK, and AFT6α

¶To whom correspondence should be addressed: frpapa@medicine.ucsf.edu (F.R.P.) and scott.oakes@ucsf.edu (S.A.O.) .
*These authors contributed equally.

Materials and methods are available as supplementary material on Science Online.

attempt to resolve ER stress through complimentary homeostatic mechanisms, which include inhibiting cap-dependent protein translation, increasing ER chaperones, and enhancing ER-associated protein degradation (ERAD) (2). However, if ER stress cannot be remedied through these mechanisms, the UPR induces apoptosis through the mitochondrial BAX/BAK-dependent pathway (1). Excessive ER stress-induced cell loss contributes to numerous human degenerative diseases, including diabetes, neurodegeneration, and cardiovascular disease (1, 3, 4)

Severe ER stress activates the protease CASPASE-2 (CASP2) as an early apoptotic switch upstream of mitochondria (3-7). Once activated, CASP2 cleaves the BH3-only protein BID, which then localizes to mitochondria to induce BAX/BAK-dependent apoptosis (8,9). However, the molecular events leading from the detection of upstream ER stress to CASP2 activation remain unknown. To address this question, we challenged wild-type (WT) and apoptosis-resistant *Bax*$^{-/-}$*Bak*$^{-/-}$ (DKO) mouse embryonic fibroblasts (MEFs) with brefeldin A (BFA), a drug that retards protein trafficking in the secretory pathway to cause ER stress. CASP2 protein, which is normally expressed at low levels in these cells, increased dramatically within 2hrs of BFA treatment and rose steadily over the next 12-18hrs (Fig. 1A,B, S1). CASP2 then underwent internal cleavage at ~18hrs, concomitant with entry of WT—but not DKO—MEFs into the apoptotic pathway, as evidenced by activation of the downstream executioner CASP3 and Annexin-V staining (Fig. 1A-C). CASP2 upregulation and activation was preserved in DKO MEFs, which suggests that it occurs upstream of the mitochondrial apoptotic pathway (Fig. 1B,C). Furthermore, CASP2 was efficiently induced by ER stress in *Atf6α*$^{-/-}$ and *Perk*$^{-/-}$, but not in *Ire1α*$^{-/-}$ MEFs (Fig. 1D, E); and CASP2-dependent proteolytic activation of BID in response to ER stress was absent in *Ire1α*$^{-/-}$ MEFs (Fig. S2). Thus, IRE1α may represent the upstream ER sensor used by cells to upregulate CASP2 protein. Consistent with this notion, *Ire1α*$^{-/-}$ MEFs were resistant to BFA-induced apoptosis, and provision of IRE1α reconstituted apoptosis in a BAX/BAK-dependent manner (Fig. S3 and S4).

IRE1α consists of an N-terminal sensor domain within the ER that detects misfolded proteins, a transmembrane region, and a cytosolic tail containing two distinct catalytic activities—a serine/threonine kinase and an endoribonuclease (RNase) (10, 11) (Fig. S7). Accumulation of misfolded proteins within the ER leads to IRE1α oligomerization and subsequent trans-autophosphorylation, which allosterically activates its RNase. Isogenic T-REx-293 cell lines have been generated that express either WT or various mutant forms of IRE1α under doxycycline (Dox) control (12). Because activation of IRE1α requires oligomerization in the ER membrane, this process can be driven by mass action in the absence of ER stress (12). Activation of WT-IRE1α was sufficient for both robust upregulation of CASP2 and its subsequent cleavage, similar to what occurs under irremediable ER stress (Fig. 2A, S5 and S6).

To determine the contribution of the kinase and/or RNase activity of IRE1α in CASP2 upregulation, we tested various IRE1α mutants (Fig S7). A kinase-active/RNase-dead variant of IRE1α (K907A) was unable to upregulate CASP2 (Fig. 2B). We employed a chemical-genetic tool that can selectively activate IRE1α's RNase, IRE1α (I642G) (12). The IRE1α (I642G) mutant is deficient in phosphotransfer activity (12, 13), but in the presence of 1NM-PP1 undergoes a conformational change that activates its RNase (12,13). Dox-induced expression of IRE1α (I642G) alone (RNase 'OFF') did not increase CASP2, but the addition of 1NM-PP1 (RNase 'ON') increased CASP2 as efficiently as WT-IRE1α (Fig 2B). Unlike under WT-IRE1α activation, there was no CASP2 cleavage after 1NM-PP1 activation of IRE1α (I642G). Thus, CASP2 is subject to multi-step regulation downstream of IRE1α, and activating the RNase of IRE1α (I642G) with 1NM-PP1 selectively activates the initial step in the process. Consistent with this notion, forcible

activation of IRE1α (I642G) does not cause apoptosis (12). IRE1α-mediated CASP2 upregulation occurred independently of its classical target, XBP1 (Fig. 2C, D, and S8).

While *Casp2* mRNA levels remained stable in response to BFA or WT-IRE1α (Fig. S9), poly-ribosome-associated *Casp2* mRNA significantly increased within 1hr of BFA in *Ire1*α$^{+/+}$ but not *Ire1*α$^{-/-}$ MEFs (Fig. 3A and S10). Moreover, CASP2 increased in response to BFA even when transcription was blocked with Actinomycin D (Fig. 3B), but not when translation was blocked with cycloheximide (Fig S11). Thus, IRE1α's RNase appears to upregulate CASP2 expression post-transcriptionally. A bioinformatic analysis of *Casp2* mRNA revealed several high confidence matches for binding sequences of known microRNAs (miRs) within its 3′-untranslated region (3′-UTR), including miR-17, miR-34a, miR-96 and miR-125b (Fig S12). These 4 miRNAs rapidly and significantly decreased in *Ire1*α$^{+/+}$ but not *Ire1*α$^{-/-}$ MEFs upon BFA treatment (Fig. 3C); while an unrelated miRNA, let-7a, did not. We could mimic this regulation using our chemical-genetic tools: WT-IRE1α or 1NM-PP1 activation of IRE1α (I642G) also caused rapid decreases in miR-17, -34a, -96, and -125b (Fig. 3D).

To test whether IRE1α-mediated reduction of select miRNAs can increase translation of a target mRNA, we devised a reporter system with an mCherry gene construct containing defined miRNA binding sites within its 3′-UTR. As such, mCherry expression is low in the presence of the matching miRNA, but becomes upregulated if the specific miRNA decreases sufficiently. The mCherry reporters for miR-17, -34a, -96, and -125b (but not let-7a) in T-REx-293 cells were all upregulated following Dox-induction of WT-IRE1α or IRE1α (I642G) plus 1NM-PP1 (Fig. S13 A, B, G-H). BFA caused similar increases in these miRNA reporters in *Ire1*α$^{+/+}$ but not *Ire1*α$^{-/-}$ MEFs (Fig. S13, C-F). To examine the role of these miRNAs in regulating *Casp2* translation, we transfected T-REx-293 cells with specific anti-miRNA oligonucleotides (14-16). Anti-miR-17, -34a, -96, or -125b each modestly increased CASP2, but all 4 together led to CASP2 levels similar to those seen with BFA (Fig. 4A). Conversely, single anti-*Casp2* miRs (-17, -34a, -96, -125b) partially reduced and the combination of all four effectively prevented CASP2 upregulation by IRE1α (Fig. 4B). To determine if the binding sequences for miR-17, -34a, 96- and -125b within the 3′-UTR of *Casp2* mRNA are critical for translational control, we introduced the complete 3′-UTR sequence into a dual Firefly (FLuc) and *Renilla* (RLuc) luciferase reporter system in the T-REx-293 cells (17). Similar to the endogenous *Casp2* mRNA, Dox-induction of WT-IRE1α or I642G-IRE1α plus 1NM-PP1 activated 3′-UTR-dependent translation as indicated by increases in the RLuc/FLuc ratio, but not when the binding sequences for the anti-*Casp2* miRNAs were mutated (Fig. S14). Thus, IRE1α controls *Casp-2* translation via downregulating these select anti-*Casp2* miRNAs.

To explore the mechanism through which IRE1α downregulates these miRNAs, we examined the biogenesis of miR-17. IRE1α activation did not affect pri-miR-17, but significantly reduced both pre-miR-17 and mature miR-17 (Fig. 4C), suggesting that IRE1α regulates its biogenesis at the precursor step. Indeed, incubation of radiolabeled pre-miR-17 with recombinant human WT IRE1α or 1NM-PPI activated IRE1α (I642G) (but not the K907A RNase mutant) resulted in two prominent fragments (~40 nt and ~17 nt), as well as a slightly less abundant ~49nt fragment (Fig. 4D). These IRE1α cleavage products all mapped to positions distinct from DICER sites but with some similarity to IRE1α's scission sites in *Xbp1* (Fig. 4E, F). Thus, IRE1α appears to cleave select pre-miRNAs directly to prevent proper DICER processing of their mature forms, a mechanism recently described for how another ribonuclease, MCPIP1, terminates miRNA biogenesis (18).

Hyperactivated WT IRE1α--but not 1NM-PP1 activated IRE1α (I642G)--endonucleolytically degrades hundreds of ER-localized mRNAs, which further compromises

ER protein-folding capacity and hastens cell demise (12). While activated WT-IRE1α and IRE1α (I642G) both decreased anti-*Casp2* miRNAs to induce expression of pro-CASP2, only the former triggered its subsequent proteolytic processing, suggesting that ER-localized mRNA decay may be a critical "second signal" for full CASP2 activation and apoptosis. Unlike mRNAs directed to the ER membrane through a signal peptide leader sequence, it is currently unclear how pre-miRNAs gain proximity to IRE1α under conditions of ER stress. Possibilities include alterations in miRNA localization structures (e.g., P-bodies, stress granules), the involvement of miRNA-binding proteins, or the loss of other miRNA protective factors (19-21). Alternatively, because the outer nuclear membrane is continuous with the ER, IRE1α may become exposed to pre-miRNAs as they transit through the nuclear pore.

There have been previous hints of a connection between miRNAs and ER stress signaling. For instance, the apoptotic proteins BIM, BAK and PUMA are known to increase during ER stress-induced apoptosis (7, 22, 23), and contain putative miRNA binding sites within their 3′-UTRs. Furthermore, we recently found that IRE1α posttranscriptionally stabilizes the mRNA encoding the pro-oxidant TXNIP in part through reducing miR-17 to activate the NLRP3 inflammasome in pancreatic beta cells under ER stress (24). Here we provide evidence that the action of IRE1α on miRNA biogenesis is direct and that it antagonizes classical processing by DICER to derepress a translational block to entry into apoptosis. Thus, endonucleolytic cleavage of miRNA precursors by IRE1α adds to a growing list of extra-Xbp1 mRNA splicing functions controlled by this UPR sensor. Given their potential to alter expression of multiple mRNA targets simultaneously, non-coding RNAs are well-suited to govern complex cellular remodeling in response to ER stress signaling.

Supplementary Material

Refer to Web version on PubMed Central for supplementary material.

Acknowledgments

We thank R. Kaufman for *Atf6α*$^{-/-}$ MEFs and D. Ron for *Perk*$^{-/-}$ and *Ire1α*$^{-/-}$ MEFs. The work was supported by NIH: DP2OD001925 (F.R.P), RO1CA136577 (S.A.O.), RO1CA136717 (A.G), RO1DK080955 (F.R.P), RO1CA154916 (D.R.), GM080783 (M.T.M.), DK063720 (M.T.M.), and RO1CA140456 (D.R.); Leukemia & Lymphoma Society Scholar Award (D.R.), Howard Hughes Medical Institute Physician-Scientist Early Career Award (S.A.O.); American Cancer Society Research Scholar Award (S.A.O.); Burroughs Wellcome Foundation (F.R.P.); Hillblom Foundation (F.R.P.); Juvenile Diabetes Research Foundation (F.R.P); Partnership for Cures (F.R.P); National Science Foundation (E.S.W.); Susan G. Komen Foundation (A.G) and an A*STAR Fellowship (L.L.). J-P.U., L. W., D. H., E.S.W., N.H., M.T. designed and performed experiments and contributed to the manuscript. L.L., M.T.M., D.R. and A.G. contributed key ideas, reagents and data interpretation. F.R.P. and S.A.O. designed the study and wrote the manuscript. There are no conflicts of interest.

REFERENCES

1. Shore GC, Papa FR, Oakes SA. Signaling cell death from the endoplasmic reticulum stress response. Curr Opin Cell Biol. 2011; 23:143–149. [PubMed: 21146390]
2. Ron D, Walter P. Signal integration in the endoplasmic reticulum unfolded protein response. Nat Rev Mol Cell Biol. 2007; 8:519–529. [PubMed: 17565364]
3. Yoshida H. ER stress and diseases. Febs J. 2007; 274:630–658. [PubMed: 17288551]
4. Reyes NA, et al. Blocking the mitochondrial apoptotic pathway preserves motor neuron viability and function in a mouse model of amyotrophic lateral sclerosis. J Clin Invest. 2010; 120:3673–3679. [PubMed: 20890041]
5. Upton JP, et al. Caspase-2 cleavage of BID is a critical apoptotic signal downstream of endoplasmic reticulum stress. Mol Cell Biol. 2008; 28:3943–3951. [PubMed: 18426910]

6. Nutt LK, Buchakjian MR, et al. Metabolic control of oocyte apoptosis mediated by 14-3-3zeta-regulated dephosphorylation of caspase-2. Dev Cell. 2009; 16(6):856–866. [PubMed: 19531356]
7. Nutt LK, Margolis SS, et al. Metabolic regulation of oocyte cell death through the CaMKII-mediated phosphorylation of caspase-2. Cell. 2005; 123(1):89–103. [PubMed: 16213215]
8. Bonzon C, Bouchier-Hayes L, Pagliari LJ, Green DR, Newmeyer DD. Caspase-2-induced apoptosis requires bid cleavage: a physiological role for bid in heat shock-induced death. Mol Biol Cell. 2006; 17:2150–2157. [PubMed: 16495337]
9. Wei MC, et al. Proapoptotic BAX and BAK: a requisite gateway to mitochondrial dysfunction and death. Science. 2001; 292:727–730. [PubMed: 11326099]
10. Tirasophon W, et al. A stress response pathway from the endoplasmic reticulum to the nucleus requires a novel bifunctional protein kinase/endoribonuclease (Ire1p) in mammalian cells. Genes & Development. 1998; 12:1812–1824. [PubMed: 9637683]
11. Wang X-Z, et al. Cloning of mammalian Ire1 reveals diversity in the ER stress responses. EMBO J. 1998; 17:5708–5717. [PubMed: 9755171]
12. Han D, et al. IRE1alpha kinase activation modes control alternate endoribonuclease outputs to determine divergent cell fates. Cell. 2009; 138:562–575. [PubMed: 19665977]
13. Papa FR, et al. Bypassing a kinase activity with an ATP-competitive drug. Science. 2003; 302:1533–1537. [PubMed: 14564015]
14. Krutzfeldt J, et al. Silencing of microRNAs in vivo with 'antagomirs'. Nature. 2005; 438:685–689. [PubMed: 16258535]
15. Vermeulen A, et al. Double-stranded regions are essential design components of potent inhibitors of RISC function. Rna. 2007; 13:723–730. [PubMed: 17400817]
16. Bartel DP. MicroRNAs: target recognition and regulatory functions. Cell. 2009; 136:215–233. [PubMed: 19167326]
17. Yekta S, et al. MicroRNA-Directed Cleavage of HOXB8 mRNA. Science. 2004; 304:594–596. [PubMed: 15105502]
18. Suzuki, Hiroshi I.; Arase, M., et al. MCPIP1 Ribonuclease Antagonizes Dicer and Terminates MicroRNA Biogenesis through Precursor MicroRNA Degradation. Molecular Cell. 2011; 44(3): 424–436. [PubMed: 22055188]
19. Almeida MI, Reis RM, et al. MicroRNA history: Discovery, recent applications, and next frontiers. Mutat Res. 2011; 30:30.
20. Long D, et al. Potent effect of target structure on microRNA function. Nat Struct Mol Biol. 2007; 14:287–294. [PubMed: 17401373]
21. Leung AK, Sharp PA. MicroRNA functions in stress responses. Mol Cell. 2010; 40:205–215. [PubMed: 20965416]
22. Puthalakath H, et al. ER Stress Triggers Apoptosis by Activating BH3-Only Protein Bim. Cell. 2007; 129:1337–1349. [PubMed: 17604722]
23. Kieran D, Woods I, et al. Deletion of the BH3-only protein puma protects motoneurons from ER stress-induced apoptosis and delays motoneuron loss in ALS mice. Proc Natl Acad Sci U S A. 2007; 104(51):20606–20611. [PubMed: 18077368]
24. Lerner AG, et al. IRE1α induces thioredoxin-interacting protein to activate the NLRP3 inflammasome and promote programmed cell death under irremediable ER stress. Cell Metab. 2012; 16(2):250–264. [PubMed: 22883233]
25. Yoon A, et al. Impaired control of IRES-mediated translation in X-linked dyskeratosis congenita. Science. 2006; 312:902–906. [PubMed: 16690864]

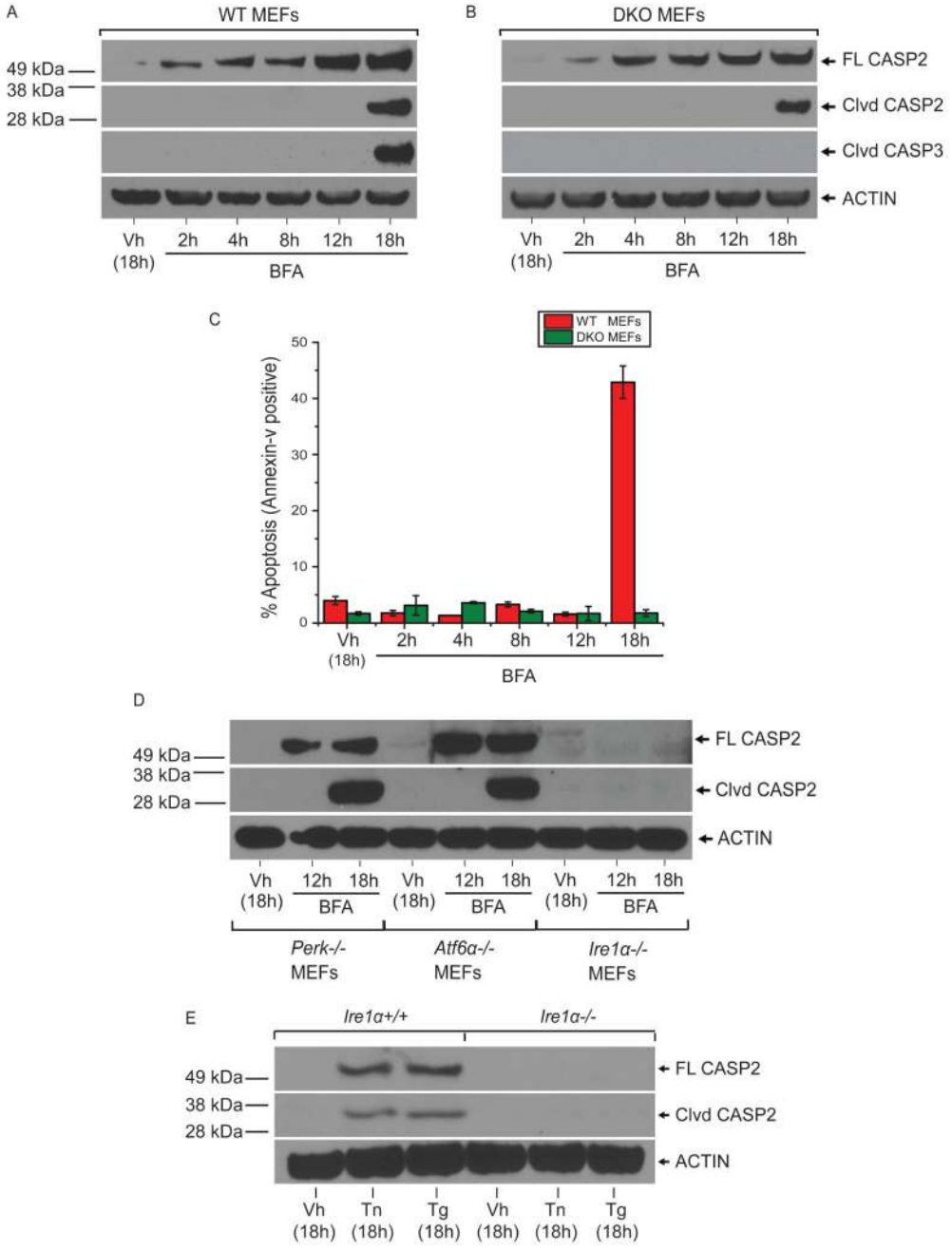

Fig. 1.

IRE1α is necessary and sufficient for CASP2 upregulation. (**A** and **B**) Immunoblot for full length (FL) CASP2 and cleaved (Clvd) CASP2 in WT and DKO MEFs after BFA treatment. (**C**) Annexin-V directed FACS analysis of WT and DKO MEFs treated with BFA. (**D**) CASP2 immunoblot in UPR sensor deficient MEFs treated with BFA. (**E**) CASP2 immunoblot of *Ire1α*$^{+/+}$ and *Ire1α* $^{-/-}$ MEFs treated with tunicamycin (Tn) or thapsigargin (Tg). Each data point represents the mean value ± SD from three independent experiments.

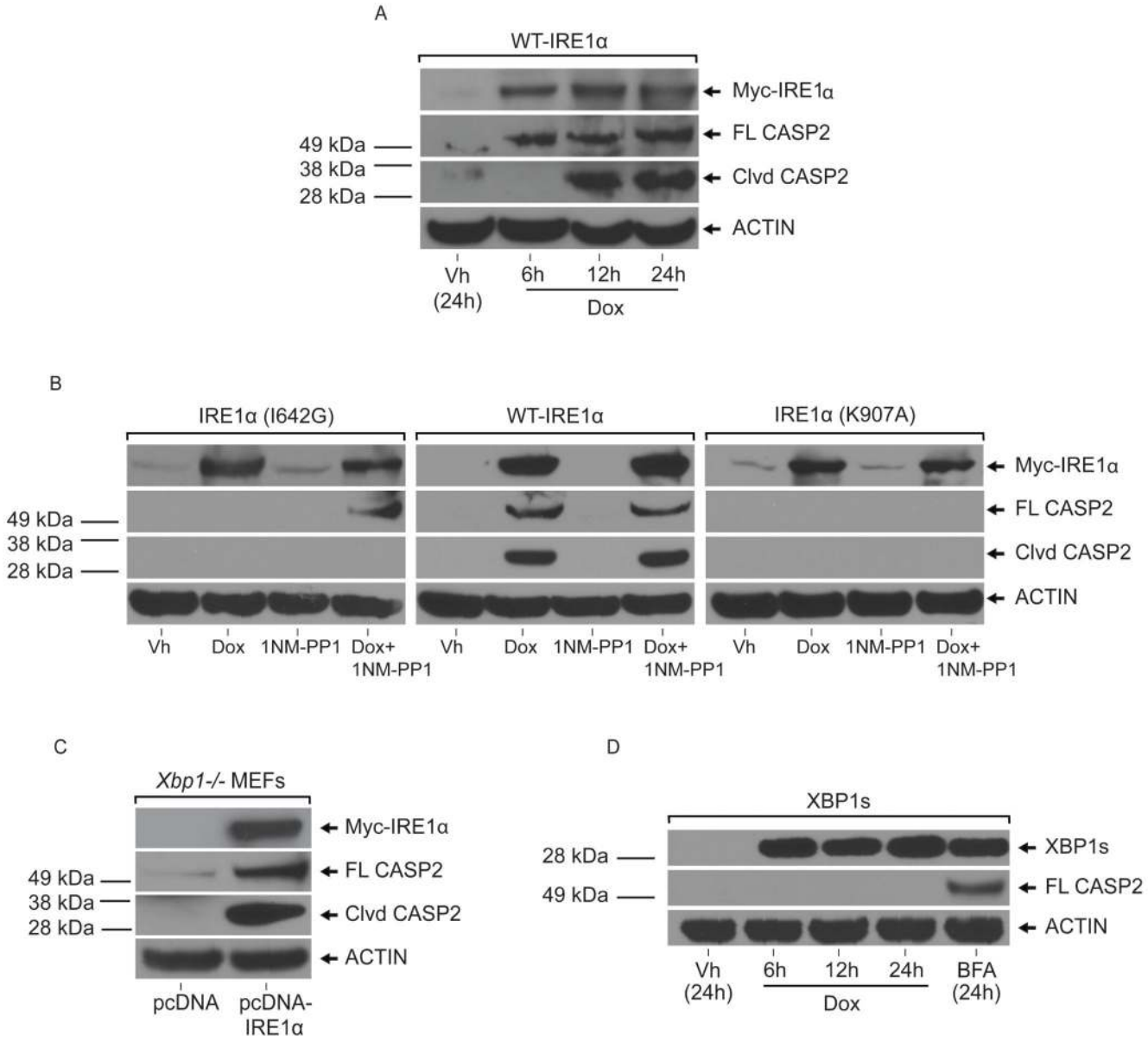

Fig. 2.

The RNase activity of IRE1α upregulates CASP2 independently of XBP1. (**A**) CASP2 immunoblot upon Dox-induction of WT-IRE1α in T-REx-293 cells. (**B**) CASP2 immunoblot in cells that over-express various IRE1α forms (**C**) CASP2 immunoblot in *Xbp1*$^{-/-}$ MEFs transfected with pcDNA5-WT-IRE1α. (**D**) CASP2 immunoblot in T-REx-293 cells before and after Dox-induction of XBP1s.

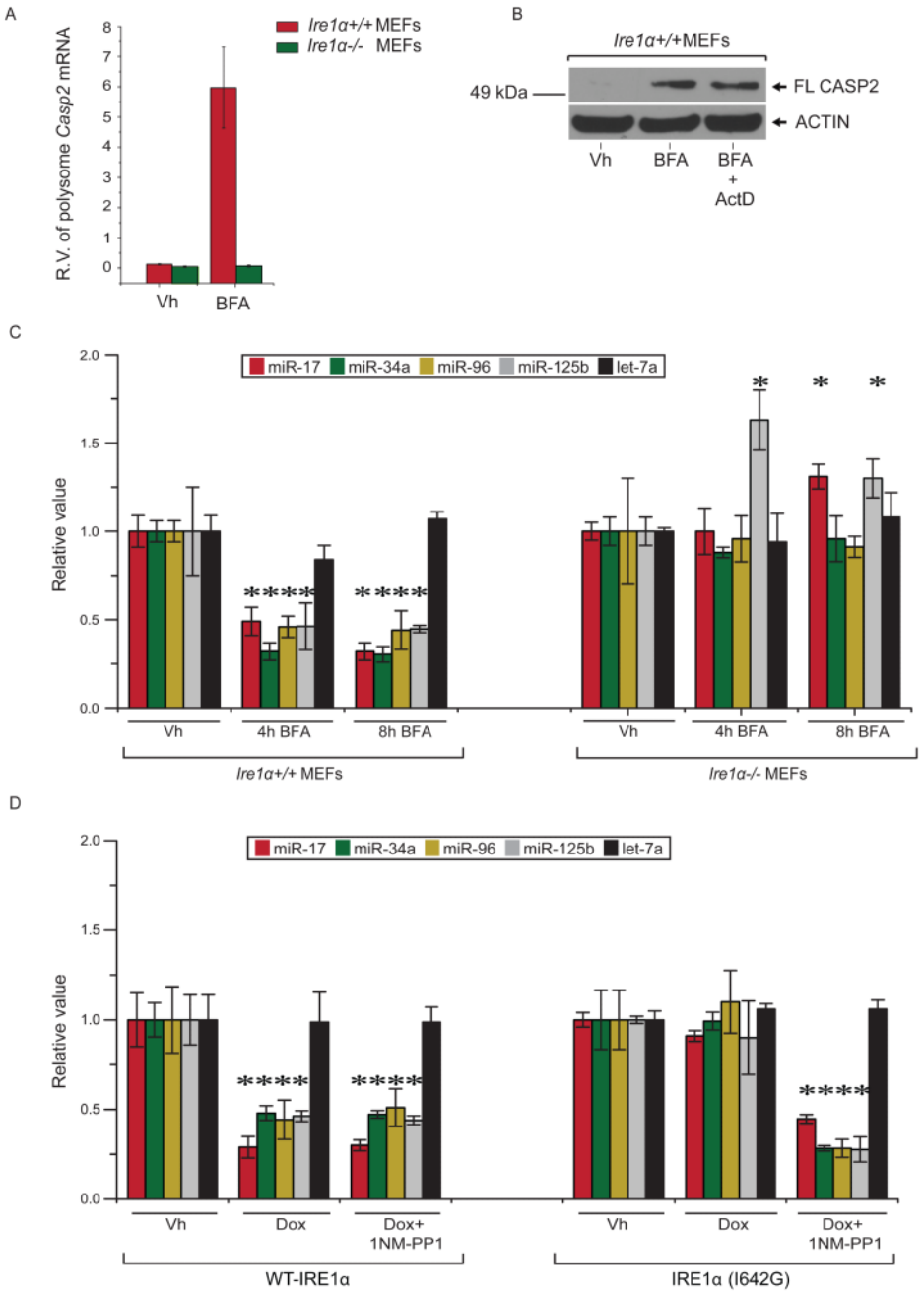

Fig. 3.

Anti-*Casp2* miRNAs decrease in IRE1α-dependent manner. (**A**) qPCR on poly-ribosome associated *Casp2* mRNA derived from *Ire1α*$^{+/+}$ and *Ire1α* $^{-/-}$ MEFs before and after BFA treatment (**B**) CASP2 Immunoblot of *Ire1α*$^{+/+}$ MEFs treated with BFA plus/minus pre-treatment with actinomycin A (ActD). qPCR of select miRNAs from (**C**) *Ire1α*$^{+/+}$ and *Ire1α* $^{-/-}$ MEFs after BFA treatment and (**D**) T-REx-293 cells after over-expression of WT-IRE1α or 1NM-PP1 activation of IRE1α (I642G). Each data point represents the mean value ± SD from three independent experiments. Asterisks indicate a statistically significant change from the vehicle treated controls ($p<0.05$).

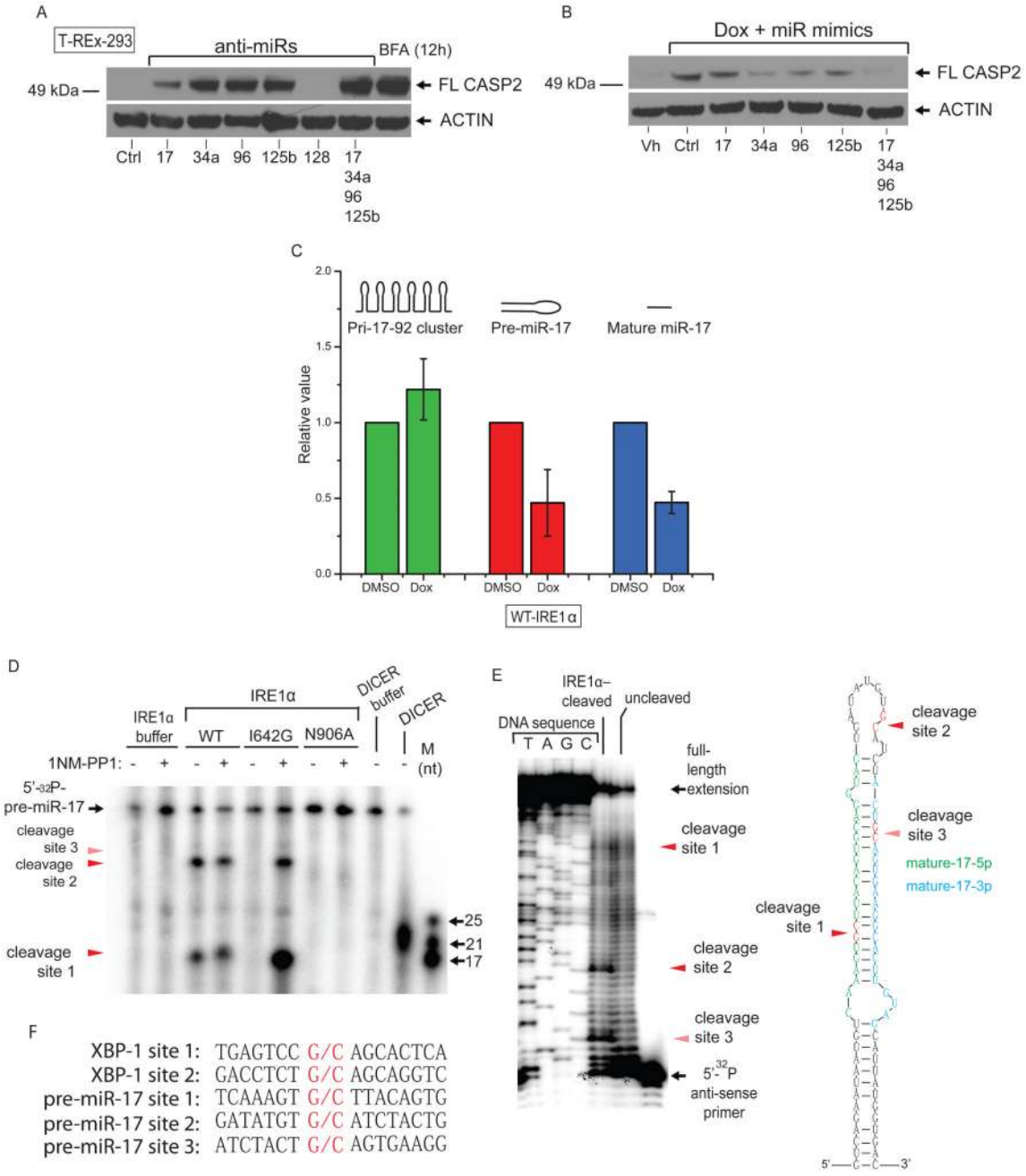

Fig. 4.

WT-IRE1α directly cleaves pre-miR-17. CASP2 immunoblot of T-REx-293 cells transfected with indicated (**A**) anti-miRNAs or (**B**) miRNA mimics after Dox-induction of WT-IRE1α. (**C**) qPCR of pri-, pre-, and mature miR-17 after IRE1α activation in WT-IRE1α T-REx-293 cells. (**D**) Radioblot of ^{32}P-labeled pre-miR-17 digestion products after incubation with indicated recombinant IRE1α proteins. (**E**) Mapping of IRE1α cleavage sites in pre-miR-17. (**F**) Illustration of the IRE1α cleavage sites within pre-miR-17. Each data point represents the mean value ± SD from three independent experiments.